Scanning Microscopy Vol. 12, No. 1, 1998 (Pages 17-29) 0891-7035/98$5.00+.25
Scanning Microscopy International, Chicago (AMF O'Hare), IL 60666 USA

THE DYNAMICS OF STEPS ON VICINAL SURFACES DURING RECONSTRUCTION-DRIVEN FACETING

H.-C. Jeong[1] and J.D. Weeks*

Institute for Physical Sciences and Technology, University of Maryland, College Park, Maryland 20742
[1]Current address: Dept. Physics, Sejong University, Kwangjin, Seoul 143-747, Korea
(Received for publication May 27, 1996 and in revised form October 9, 1996)

Abstract

Experiments show that faceting of a vicinal surface can be driven by surface reconstruction, which often occurs only on sufficiently wide terraces. We study the dynamics of steps near an isolated reconstructed terrace using a simple one-dimensional model that assigns a lower free energy (due to reconstruction) for terraces with width greater than some critical width w_c. When mass is conserved locally, through surface diffusion, we find that the growth of a reconstructed terrace can induce the growth of another such terrace nearby. This induced nucleation process is analyzed using a simple and physically suggestive picture where analytic results can be obtained. The faceted surfaces arising from this process are predicted to have a periodic distribution of reconstructed terraces separated by step bunches. The long time behavior of the faceting is obtained using a scaling ansatz. A similar analysis is carried out for the non-conserved case.

Key Words: Surface steps, periodic facet patterns, dynamics, surface reconstruction, induced nucleation.

*Address for correspondence:
J.D. Weeks
Institute for Physical Science and Technology
University of Maryland
College Park, MD 20742–2431
Telephone number: (301) 405–4802
FAX number: (301) 314–9404
E-mail: jdw@ipst.umd.edu

Introduction

Surface reconstruction can often cause a vicinal surface with a single macroscopic orientation to facet into surfaces with different orientations [18]. Generally the reconstruction occurs on a particular low index "flat" face, and lowers its free energy relative to that of an unreconstructed surface with the same orientation. However the same reconstruction that produces the lower free energy for the flat face generally **increases** the energy of surface distortions such as steps which disturb the reconstruction. Thus, reconstruction is often observed only on terraces wider than some critical terrace width w_c. When steps are uniformly distributed initially and if w_c is much greater than the average terrace spacing w_a, step fluctuations leading to the formation of a sufficiently wide terrace, a "critical nucleus", are required for the reconstruction to begin. Continued growth of the reconstructed region can make the vicinal surface facet into a "flat" reconstructed surface and a much more sharply inclined unreconstructed surface with closely bunched steps. In this paper, we examine the dynamics of faceting after such an initial nucleation event.

Experimental examples include the 7×7 reconstruction on Si(111) surfaces [12] and the formation of (n×1) oxygen chains on an O/Ag(110) surface [11]. Both have been observed only on large ($w>w_c$) terraces, where the critical width w_c depends on temperature, pressure and some other parameters. However, faceting experiments on these and some other systems, such as Pt(111) and Au(111), show a noticeable regularity in the size and spacing of the flat facets [12, 15, 19] though the extent of regularity is different depending on the system. It seems hard to reconcile these regularities with a picture of random nucleation of the reconstructed regions.

While there are a number of different factors (including, in particular, elastic interactions [15, 19]) that can contribute to the facet spacing in particular systems, we argue that there exists a rather general **kinetic** mechanism that can lead to regular features in the faceting process. This mechanism may, in part, explain some aspects of the regularity found in recent experiments.

We consider the case where the reconstruction effectively occurs only on terraces wider than some critical terrace width w_c, and assign a lower free energy (due to

reconstruction) for terraces wider than w_c. If w_c is much greater than the initial average terrace spacing w_a, a nucleation event is required to form the first wide terrace. The subsequent temporal and spatial behavior of the faceting process depends crucially on the mechanism of mass transport on the surface. When mass transport is **global**, through a reservoir, as in the case of evaporation and condensation, the nucleated facet continues to grow indefinitely in the absence of another nearby thermal nucleation event. All neighboring terraces become smaller as the reconstructed facet grows and this makes nucleation near the growing facet **less** likely.

However, when mass transport is **local**, as in mass movement through surface diffusion without direct ad-atom hops between terraces, we find the facet does not continue to grow indefinitely. In this case, the motion of a step is directly coupled to the motion of neighboring steps. Because of this coupling, a growing nucleus can **induce** the formation of another nucleus nearby [3, 4] which "collides" with the original facet. This can lead to a propagation of nucleation events [6]. The faceted surface formed in this **induced nucleation** process exhibit very different characteristics from the conventional thermally nucleated one. In this process, the average number of steps in a bunch, n_b, and final facet size, W_f, are mainly selected by the kinetics.

Model

We concentrate on the kinetics of faceting on a vicinal surface after the initial formation of a reconstructed critical nucleus. We assume that reconstruction occurs quickly once a suitable terrace is formed. In most cases, once such a nucleus is created, it propagates much faster in the direction parallel to the steps and quickly forms an elongated cigar like shape. The steps which bound the lateral regions of the elongated nucleus are usually almost straight [12]. Thus, it seems plausible that the growth of the nucleated facet in the direction **perpen-dicular** to the steps can be well described by a one-dimensional (1D) terrace step (TS) model, even though it cannot describe the initial two-dimensional (2D) nucleation event itself. The 1D variable, the position of the nth step x_n in our TS model is the coarse grained **average** (over the lateral size L_y of the elongated nucleus) position of the nth step.

The projected free-energy density (this is the free energy per unit **projected** surface area; use of the projected free energy allows a direct analogy to the phase separation dynamics of a liquid-vapor system [18]) of a vicinal surface inclined at an average angle θ to the low-index reference plane on which reconstruction can occur (referred to hereafter as the flat surface) is well described by [2, 5, 14, 17, 18]

$$f_{r,u}(s) = f_{r,u}{}^{0} + \beta_{r,u} s + g_{r,u} s^3 \qquad (1)$$

Here s is the density of steps, which is proportional to the slope of the surface, tan θ, and the subscripts u and r indicate a surface that is **completely** unreconstructed (u) or reconstructed (r). The first term, f^0, is the surface energy per unit area of the flat surface and β is the free energy per unit length to form an isolated step. The last term is the free energy due to the effective interactions between the steps. This term includes the entropic repulsion between steps (due to fluctuations along the step edge) as well as possible energetic contributions such as elastic or dipole interactions [10]. In most cases, the effective interaction between steps of the same sign is repulsive ($g > 0$). Hence, the free energy of the vicinal surface, $f_{r,u}$, is convex downward (as shown in Fig. 1). Therefore, the vicinal surface of a single phase (either completely unreconstructed or reconstructed) is stable with respect to faceting.

Reconstruction induced faceting naturally arises if surface reconstruction occurs only on large $w > w_c$ terraces. This means that f_r is smaller than f_u for $s < s_c \equiv 1/w_c$ but that f_r

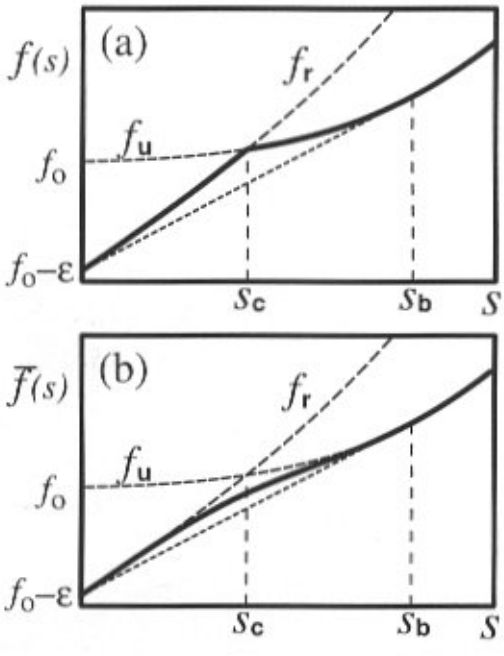

Figure 1. Free energies for the unreconstructed surface f_u and reconstructed surface f_r versus slope s. The critical slope, s_c, and the slope of the surface at step bunches, s_b, are given by $s_c = \varepsilon_s/\varepsilon$ and $s_b = (\varepsilon/2g)^{1/3}$. The thick curve in (**a**) represents the free energy of a hypothetical system in which all terraces are reconstructed (unreconstructed) when the average slope, s, is less than (greater than) s_c. In (**b**), a free-energy curve is shown which takes into account a distribution of terrace widths. The free Fermion model is used to get the distribution for a given s.

is larger than f_u for $s > s_c$. As discussed earlier, this can be understood by assuming that the free energy of the reconstructed flat surface has a lower value ($-\varepsilon$ per unit area; $f_r^0 = f_u^0 - \varepsilon$) than the unreconstructed flat surface but effectively a higher energy cost (ε_s per unit length; $\beta_r = \beta_u + \varepsilon_s$) for forming an isolated step [17]. The critical slope s_c is then given by $s_c = \varepsilon_s/\varepsilon$ as shown in Figure 1. The thick curve in Figure 1a, given by

$$f(s) = f_u(s)\boldsymbol{\theta}(s - s_c) + f_r(s)\boldsymbol{\theta}(s_c - s) = f_u(s) - (1 - s/s_c)\varepsilon\boldsymbol{\theta}(s - s_c) \quad (2)$$

with $\boldsymbol{\theta}$ the unit step function, represents the free energy of a hypothetical system in which **all** terraces are reconstructed (unreconstructed) when the average slope s is less than (greater than) s_c. (For simplicity, we use the same value of g for the reconstructed and unreconstructed surfaces. The change in g, Δg, between the two surfaces does not play an important role in what follows.) As in earlier work [9, 13], we assume this same expression can be applied **locally** to give $\tilde{f}(w)$, the free energy of an **individual** terrace with width $w = 1/s$. Thus, we assume $\tilde{f}(w) = f(1/w)$, even in cases where adjacent terrace widths vary. This yields a simple two state model where each terrace is either reconstructed or unreconstructed, depending only on its width.

In a real system, for given average slope s, there would be a distribution of terrace widths around the average terrace width $w = 1/s$. Near s_c, we would expect to find both reconstructed and unreconstructed terraces in a large system. This would remove the cusp at s_c in $f(s)$ and produce a smoothly varying curve in this region. In Figure 1b, a modified free energy curve is shown, which takes into account, in a crude way, a distribution of terrace widths. The free Fermion model [5] is used to get the distribution of widths. For a given s, the relative number of terraces of which the width is larger than w_c and their relative area are calculated [7]. We assume that reconstruction takes place on all of these wide terraces and takes into account the resulting free-energy change to determine a new $\tilde{f}(s)$. As expected, this removes the cusp at s_c in Eq. (2) and produces a smooth free-energy curve.

However, in either model, the free energy of the combined system loses overall convexity, and the uniform system is unstable. Thus, "phase separation" occurs between the two "phases" of which the properties are determined by the usual tie bar construction (as indicated by the dashed line in Figure 1). In particular, the slope of the step bunches coexist-ing with the reconstructed flat surface is given by $s_b \equiv (\varepsilon/2g)^{1/3}$ as shown in Figure 1. Note that the curve in Figure 1b is a coarse- grained free energy resulting from an average over many terrace widths. The free energy of an **individual** terrace near the elongated nucleus is more properly described by the curve in Figure 1a.

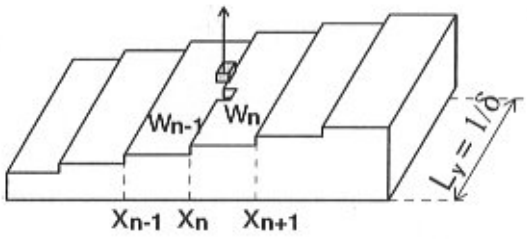

Figure 2. Labeling of steps and terraces. The chemical potential, ξ_n, of step ***n*** is defined as the difference in the total surface free energy before and after an atom is removed from step ***n***.

Kinetics

In the previous section, we showed that surface reconstruction can cause a faceting on a vicinal surface and obtained the equilibrium slopes of the faceted surfaces from thermo-dynamic arguments. However, this does not explain the spatial distribution of terraces and step bunches. The key factor in determining the sizes of the final facets is how far the facet nuclei are from each other when they form (or how often they are created when facets grow slowly compared to the creation of a nuclei). This requires a study of the **kinetics** of step motion as influenced by the attachment/detachment kinetics of atoms at the step edges. This in turn can be related to the chemical potential at the step edge [9].

The chemical potential, ξ_n, of step n (which separates the n-1 and the nth terrace; see Figure 2) is de-fined as the difference in the total surface free energy before and after an atom is removed from step n. We assume that the free-energy density on a terrace with width w can be approximated by $\tilde{f}(w) = f(1/w)$. Then, ξ_n is given by

$$\begin{aligned}\xi_n &= \{F(w_n)+F(w_{n-1})\}-\{F(w_n')+[F(w_{n-1}')\} \\ &= L_y[\{w_n\tilde{f}(w_n)-(w_n-\boldsymbol{\delta})\tilde{f}(w_n-\boldsymbol{\delta})\} \\ &\quad + \{w_{n-1}\tilde{f}(w_{n-1})-(w_{n-1}+\boldsymbol{\delta})\tilde{f}(w_{n-1}+\boldsymbol{\delta})\}] \\ &\approx \partial_\omega(w\tilde{f}(w))\big|_{wn} - \partial_\omega(w\tilde{f}(w))\big|_{wn-1}\end{aligned} \quad (3)$$

Here w_n (w_n') is the average distance between step n and n+1 before (after) an atom is removed from the step, $L_y = 1/\delta$ is the length of a step edge (i.e., the lateral size of the facet), and $F(w_n) \equiv L_y w_n \tilde{f}(w_n)$ is the surface free energy of the nth terrace. When we assume that the reconstruction effectively occurs only when a given terrace is wider than some w_c, $\tilde{f}(w_n)$ can be

accurately approximated as in Eq. (2):

$$\tilde{f}(w_n) = \tilde{f}_U(w_n) - (1 - w_c/w_n)\varepsilon\theta(w_n - w_c) \quad (4)$$

As mentioned in the previous section, the use of a critical width model for the reconstruction of an **individual** terrace as in Eq. (4) is more accurate than is the use of the uniform terrace approximation to describe $f(s)$ as in Eq. (2). The latter is inaccurate near s_c as shown in Figure 1b.

From Eqs. (3) and (4), the chemical potential ξ_n of step n is given by

$$\xi_n = [(2g/w^3_{n-1}) - (2g/w^3_n) + \varepsilon\{\theta(w_{n-1} - w_c) - \theta(w_n - w_c)\}] \quad (5)$$

We now assume that the velocity of a step is proportional to the change in free energy produced by its motion [9]. Recall that the motion of steps results from the movement of atoms at steps. Therefore, the step kinetics depends on the mechanism of mass transport on the surface. There are two limiting cases, depending on whether the adatoms on each terrace obey a local conservation condition.

The mass is **not locally conserved** (case I) when atoms at a step edge exchange with a vapor reservoir (evaporation condensation) or with a terrace reservoir that forms by fast direct adatom hops between different terraces. In either case, steps move according to the chemical potential difference between the step and the reservoir:

$$\partial_t x_n = D_r(\xi_n - \xi_{res}) \quad (6)$$

where D_r is an effective step reservoir exchange coefficient. The chemical potential of the reservoir ξ_{res} is set at zero when there is no net motion of steps. Note that the mass movement is effectively non-local since an atom from a given step can go to distant steps through the reservoir. Thus, no direct correlation between the motion of neighboring steps is expected.

However, when the mass movement is **locally conserved** (case II), as in mass movement through surface diffusion without direct adatom hops between terraces, the current between step n and step n+1 is proportional to (ξ_n - ξ_{n+1}). Thus, the net velocity of step n is

$$\partial_t x_n = D_s\{(\xi_n - \xi_{n+1}) + (\xi_n - \xi_{n-1})\} \quad (7)$$

where D_s is some effective diffusion coefficient between neighboring steps. (We follow reference [9], assuming D_s is independent of the terrace width, and neglecting possible "Schwoebel" asymmetries. Rettori and Villain [16] used a diffusion coefficient which is proportional to the inverse of the terrace width. The main results of our work, the existence of induced nucleation, holds for both cases.) This causes a **coupling** of the motion of neighboring steps and, as we will see, can lead to induced nucleation.

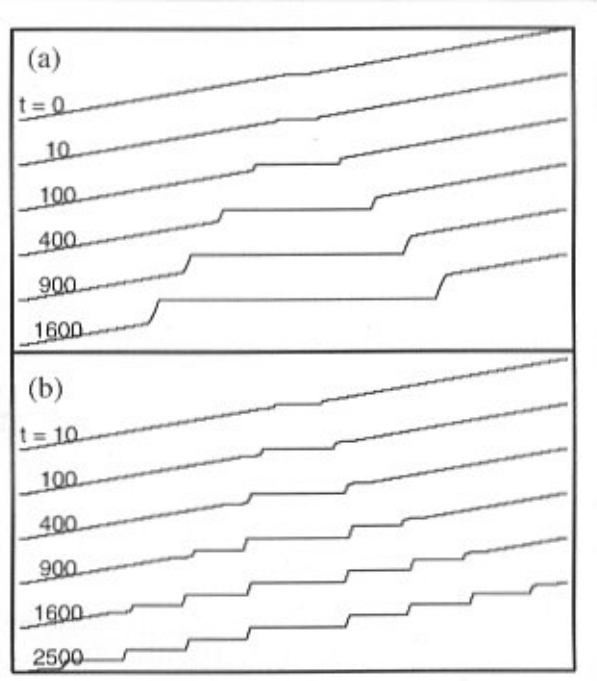

Figure 3. Surface profiles at different times in case I (**a**), and in case II (**b**). (**a**) At $t = 0$ (top one), there is only one terrace which is wider than w_c (in the middle). The other terraces are uniform with width $w_a < w_c$. (**b**) At $t = 0$ (not shown), the configuration is the same as in (a) but the evolution of the surface profile is very **dif-ferent** from that in case I. In this case, a growing flat facet induces a new nucleus for another flat facet. Here, $w_b/w_a = 1/20$ and $w_c/w_a = 3$.

Growth of the Reconstructed Terrace

Let us consider the case where only one (thermally nucleated) terrace is larger than w_c at time $t = 0$. The surface profiles at $t > 0$ are obtained by (numerically) integrating the differential Eqs. (6) and (7) with ξ_n given by Eq. (5). For case I, as shown in Figure 2a, the nucleated facet continues to grow indefinitely. The width of the facet increases as $t^{1/2}$ [8], as shown in the **Appendix**, and all neighboring terraces become smaller. Thus, further nucleation near the growing terrace is less likely.

On the other hand, for case II, the facet does not continue to grow indefinitely, in contrast to what simple thermodynamic consideration would predict [12]. Rather, it grows only to a certain size and stays there (Fig. 2b). This is because the local mass conservation causes a growing facet to **induce** a new nucleus which "collides" with the original

facet as it grows.

To understand this process, we first consider the motion of steps in the initial stages of faceting near the original reconstructed terrace. Let the origin be the middle of this "zeroth" terrace as shown in Figure 3. We assume the system is in the nucleation regime with $w_a < w_c$, and first consider the simplest case, the early stages of the faceting with $w_b << w_a$, where $w_b = 1/s_b$ is the spacing between steps in a bunch at $t = \infty$. This implies $\varepsilon >> p_a$ where $p(w_a) \equiv p_a = 2g/w_a^3$ is the repulsive "pressure" between steps with the average spacing. In this case, ε sets the relevant time and energy scales for the faceting and step repulsions play an important role in the kinetics only when the spacing w approaches w_b and $p(w) \approx \varepsilon$.

With Local Conservation

Zeroth order picture and induced nucleation

Let us consider the behavior of steps for case II first. We will see that there is a quasi-steady state in which step 1,···,n form an effective bunch of size n. All these steps move right with essentially the same velocity for some time interval, t_n-t_{n-1} for each given $n > 0$.

At $t = 0$, all terraces except the zeroth one are smaller than the critical width ($w_n = w_a < w_c$ for $n \geq 1$). The chemical potential at the nth step, ξ_n, given by Eq. (5), is zero for $n \geq 2$ and is approximately $\tilde{\varepsilon} \equiv \varepsilon - p_a$ at step 1 since the repulsion from step 2 is p_a. (We ignore the repulsion from step 0 which is even smaller than p_a.) Since $\xi_1 > \xi_2$, atoms move from step 1 to step 2, allowing the facet to grow. Thus, step 1 moves right and step 2 moves **left**, i.e., w_1 decreases and w_2 **increases**. This contrasts with the behavior in the non-conserved case (see next subsection), where all steps move to the right and only w_0 increases.

Because this movement also produces an increased repulsive interaction between step 1 and 2, ξ_2 increases a little and becomes higher than ξ_3. Although some atoms at step 2 can then move to step 3, the net motion of step 2 is still to the left as long as $(\xi_1 - \xi_2) > (\xi_2 - \xi_3)$: more atoms come from step 1 than go to step 3. However, as time goes on (and ξ_2 continues to increase while ξ_1 decreases), $(\xi_1 - \xi_2)$ eventually becomes smaller than $(\xi_2 - \xi_3)$. **Both** step 1 and step 2 now move to the **right** and w_2 now **decreases**. This occurs when the repulsive interaction between step 1 and step 2 becomes large enough to drive step 2 to the right; the spacing between the two steps is then of order w_b. Both steps 1 and 2 move right with essentially the same velocity as the facet continues to expand.

Figure 4a shows x_n, the position of step n, as a function of time t. We define the **collision time** t_1 as the time at which step 2 first begins to move to the right. Since $\varepsilon >> p_a$, step 3 has barely moved for $t < t_1$. If we ignore this small change, we have the following **zeroth order picture** where analytical results can be obtained. Step 1 moves right with a constant velocity, V_1, and step 2 moves left with another constant velocity until

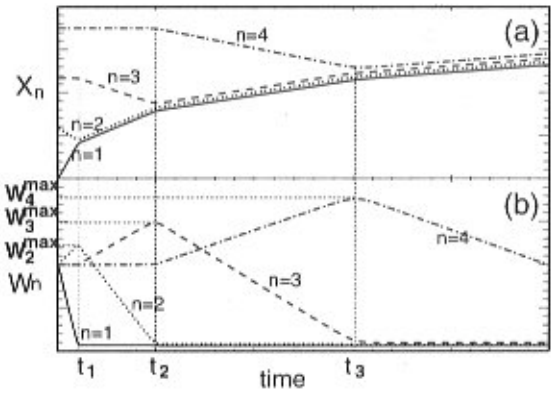

Figure 4. The step positions and the terrace widths as a function of time. Here $w_b/w_a = 1/20$. Recall that $w_n = x_{n+1}$-x_n when comparing (**a**) and (**b**).

---

they collide at $t = t_1$. The sys-tem then quickly achieves a quasi-steady state where both steps 1 and 2 move right with a smaller constant velocity, V_2. Now atoms from both steps- 1 and 2 effectively contribute to the motion of step 3, which moves left until it collides with step 2 (at $t = t_2$). For $t > t_2$, steps 1, 2 **and** 3 move right with the velocity, V_3, while step 4 moves left, and so on. Hence, in this simple limit, all terraces at any given time t, can be categorized into five groups: (**1**) the reconstructed growing terrace (terrace 0); (**2**) the terraces in the bunch which move together with the velocity V_n (terrace 1,···,n-1); (**3**) a terrace of which the width is rapidly decreasing to join the bunch (terrace n); (**4**) a terrace of which the width is increasing due to local conservation (terrace n+1); and (**5**) the remaining unperturbed terraces with initial terrace width w_a (terrace n+2,···). Note that only two consecutive terraces, terraces n and n+1, change their widths rapidly during the time interval $t_{n+1} - t_n$.

As shown in the **Appendix**, the velocity of steps 1,···,n for $t_{n-1} < t < t_n$ is given by

$$V_n = 6(2n+1)D_s\varepsilon/\{n(n^3+2n^2+2n+1)\} \qquad (8)$$

in the zeroth order picture. Since $V_n \sim n^3$ for large n, we expect t_n-$t_{n-1} \sim 1/V_n \sim n^3$ and, therefore, $t_n \sim n^4$. On the other hand, the width of the zeroth terrace at $t = t_n$ is proportional to n since there are n steps in the step bunch. Thus, in the absence of other nucleation events, we have $w_0(t_n) \sim n \sim t_n^{1/4}$, in agreement with the classic continuum treatment of Mullins [8]. A detailed calculation (**Appendix**) shows that

$$w_0(t) \approx (4/3)(72D_s\varepsilon)^{1/4}(\tilde{w})^{3/4}\, t^{1/4} \qquad (9)$$

in the absence of another nucleation event where $\tilde{w} = w_a$-w_b.

Figure 4b shows the widths of the first four terraces as a function of time. As explained, for $t < t_1$, w_1 decreases while w_0 (not shown) and w_2 increase. For $t_{n-1} < t < t_n$, w_n decreases while w_{n+1} increases. Hence, w_n has its maxi-mum, w_n^{max} at $t = t_{n-1}$. In the zeroth order picture, w_n^{max} and t_n satisfy the following equations

$$w_n^{max} = w_a + \frac{2n-1}{3n-2}\left[\sum_{k=1}^{n-1}\frac{\tilde{w}k}{2k+1} + \sum_{k=2}^{n-1}\frac{w_k^{max}-w_a}{4k^2-1}\right],$$
$$t_n = t_{n-1} + w_n^{max}/\left[V_n\left(1+n^2/(2n+1)\right)\right]. \qquad (10)$$

For large n, w_n^{max} increases **linearly** with n $\{w_n^{max} \approx (\tilde{w}/3)n\}$ and t_n increases as n^4 $\{t_n \approx \tilde{w}/(18D_s\varepsilon)\, n^4\}$. Note that there is a large time interval $\Delta t_n^{max} \sim (w_n^{max})^3$ around t_{n-1} where terrace n is larger than any of its neighbors.

One important physical implication of this observation is that new nuclei for reconstruction can be **induced** by a growing nucleus. Since w_n^{max} increases with n, for any given critical terrace width, w_c, there is an integer n such that $w_n^{max} > w_c$. Let n_b be the smallest n such that $w_n^{max} > w_c$. Once w_{nb} gets larger than w_c, reconstruction can occur. As w_{nb} continues to grow, it will induce another nucleus at $2n_b$. Then, w_{2nb} will induce w_{3nb} and so on (see Fig. 3c). All flat facet sizes (W_f) {all step bunch sizes (W_b)} are essentially the same and given by $W_f \approx n_b\tilde{w}$ $\{W_b \approx (n_b\text{-}1)w_b\}$ since the nuclei are separated by the same number of steps, n_b. The velocity of the nucleation front is **linear** in t because it always takes the same amount of time to induce a nucleus. This propagation is much faster than the conventional faceting through surface diffusion ($\sim t^{1/4}$) or through evaporation condensation ($\sim t^{1/2}$) [8].

In real materials, this kinetic facet size selection would not be sharp due to thermal fluctuations. However, in the zeroth order approximation, aside from the original facet, only one terrace is larger than w_a at a given time. As n and hence w_n^{max} increase, there is an increasing long interval Δt_n^{max} where terrace n is larger than any others due to the induced nucleation mechanism. A thermal fluctuation leading to a width $w > w_c$ is more likely to occur on such a wide terrace. Thus, even when thermal fluctuations contribute to achieving a width $w_n > w_c$, this is most likely to happen on that largest terrace and probably when w_n^{max} is close to w_c.

The width distribution in front of the growing facet can be obtained in the zeroth approximation. For each quasi-steady state, $t_{n-1} < t < t_n$, in which the steps in the bunch, steps 1,···,n, move together with the same velocity, V_n, we have

$$2\xi_k - \xi_{k+1} - \xi_{k-1} = V_n \qquad (11)$$

for all $k < n$. There is a boundary condition $\xi_{n+1} = 0$, but, the other boundary condition at $k = 0$ depends on how the reconstructed facet nucleated. For a thermally nucleated facet at step 0, we expect the chemical potential to satisfy $\xi_0 = -\xi_1$ due to symmetry. However, for an **induced** facet, there is no flux across the reconstructed terrace. Therefore, the effective chemical potential at step 0 is given by $\xi_0 = \xi_1$. As calculated in the **Appendix**, terrace widths are given by

$$w_k = w_b\{1+h_1(n)k\text{-}h_2(n)k^2+h_3(n)k^3\}^{-1/3}, \qquad (12)$$

for the $\xi_0 = -\xi_1$ case, where $h_i(n)$ is defined in the **Appendix**. If there is no net flux across the zeroth terrace ($\xi_0 = \xi_1$),

$$w(k) = w_b\left[1 - \frac{(3n^2+3n+1)\tilde{e}k}{n(n+1)(2n+1)} + \frac{\tilde{e}k^3}{n(n+1)(2n+1)}\right]^{-1/3}, \qquad (13)$$

where $\tilde{e} = \tilde{\varepsilon}/\varepsilon = \{1\text{-}(w_b/w_a)^3\}$.

Long time behavior and scaling

This simple zeroth order picture must certainly break down if w_{n-1} calculated in the nth quasisteady state from eqs. (12) and (13) becomes of order w_a. The repulsive interaction from step n+1 should then be taken into account even in the initial motion of step n. However, even for late times with $t > t_{n_c}$, where $w_{n_c-1}(t_{n_c}) \approx w_a$, it seems reasonable to assume that the steps **near** the growing reconstructed terrace (with $k << n_c$) have the same velocity. We will use this observation and simple scaling arguments to obtain the time dependent widths of terraces in the bunch next to a growing facet. These are compared with direct numerical integration and may be useful in interpreting experiments.

We assume the terrace widths near the facet are still given by Eqs. (12) and (13) with some monotonically increasing function $n(t)$. We further assume that the front of the step bunch propagates with a simple power of time, i.e., $n(t) = v^{\dagger}t^{\beta}$. Then, as t goes to infinity, the terrace widths are functions of one scaling variable $v \equiv kt^{-\beta}$;

$$w(v) = w_b\left[1 - \frac{3\tilde{e}}{v^{\dagger 2}}v^2 + \frac{2\tilde{e}}{v^{\dagger 3}}v^3\right]^{-1/3}, \qquad (14)$$

for the $\xi_0 = -\xi_1$ case, and

$$w(v) = w_b\left[1 - \frac{3\tilde{e}}{2v^{\dagger}}v + \frac{\tilde{e}}{2v^{\dagger 3}}v^3\right]^{-1/3} \qquad (15)$$

for the $\xi_0 = \xi_1$ case. We can show that β must be ¼ by calculating $\partial_t w_k$ from Eq. (7) with $w(k,t) = w(kt^{\beta})$. Since the change in the scaling variable dv for the given finite Δk becomes infinitesimally small as t goes to infinity ($dv = \Delta k t^{-1/2}$), it is natural to treat v as a continuous variable at sufficiently late

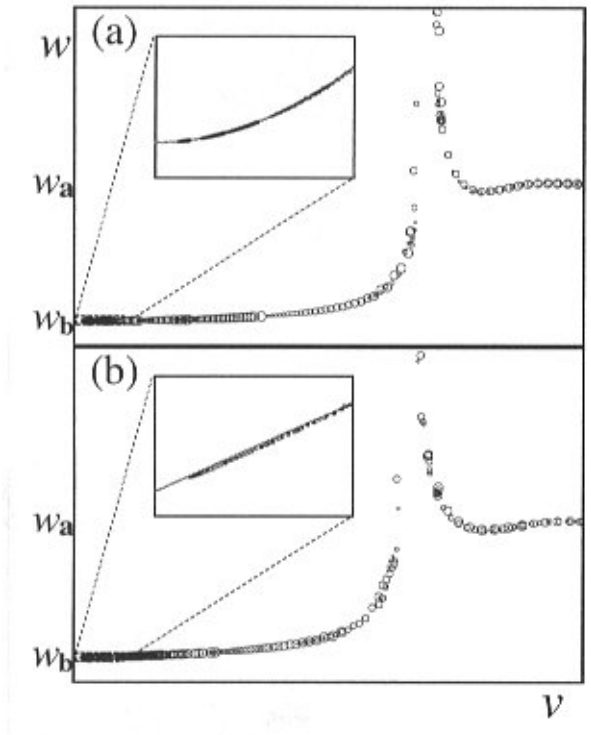

Figure 5. Terrace widths as a function of the scaling variable, $v = kt^{-\beta}$ with $\beta = 1/4$ for $w_b/w_a = 1/10$. The small v behavior is shown in the insets. Terrace widths with ten different times are shown in each panel. Clearly, all of them collapse to a single curve. The smaller circles represent the later times. For the $\xi_0 = -\xi_1$ case (**a**), the terrace width increases quadratically for small v while it increases linearly in the $\xi_0 = \xi_1$ case (**b**). The solid lines in insets are given by $w_b + c_1 v^2$ in (a) and $w_b + c_2 v$ in (b) where c_1 and c_2 are constants chosen to best fit the data.

times.

Figure 5 shows the terrace widths as a function of v. Terrace widths with ten different times (smaller circle, later time) are shown in each panel. The widths at different times clearly collapse to a single curve, indicating the high accuracy of the scaling assumption. For small v, the terrace width increases **quadratically** in Figure 5a while it is **linear** in Figure 5b as predicted from Eqs. (14) and (15);

$$w(v) \approx \quad w_b\left(1+\frac{\tilde{e}}{v^{\dagger 2}}v^2\right) \quad \text{for} \quad \xi_0 = -\xi_1,$$
$$w(v) \approx \quad w_b\left(1+\frac{\tilde{e}}{2v^{\dagger}}v\right) \quad \text{for} \quad \xi_0 = \xi_1 \qquad (16)$$

Hence, by measuring the terrace widths near the growing facet

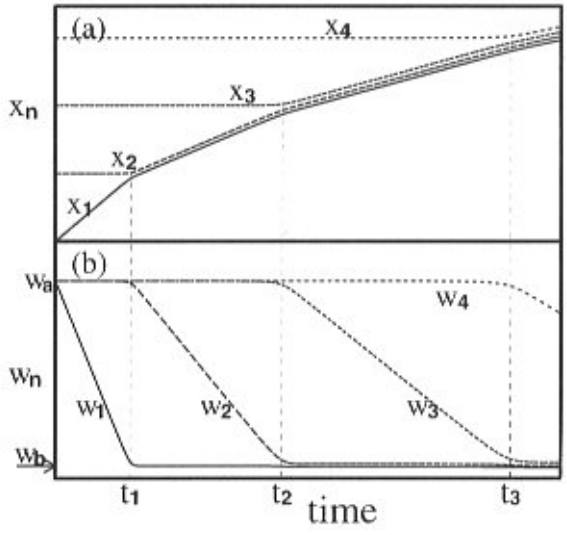

Figure 6. The step positions and the terrace widths as a function of time. Here $w_b/w_a = 1/20$. Recall that $w_n = x_{n+1} - x_n$ when comparing Figures **6a** and **6b**.

at sufficiently long times (small v), we can tell whether there is net flux across the reconstructed terrace.

Without Local Conservation

Zeroth order picture and quasi-steady state

In this sub-section, we again consider the simplest limiting case, the early stages of faceting in the non-conserved case with $w_b << w_a$ and obtain the terrace widths near the growing facet. We start with the same configuration as in the locally conserved case. As shown in Figure 6, a quasi-steady state also exists here, where all steps in the bunch, steps 1,···,n move right with essentially the same velocity, V_n. However, in this case, there is no step which moves left (backwards). Instead, step n+1 barely moves to the right from its initial position until the step n "collides" with it and pushes it rapidly to the right. Then, the system quickly achieves a new quasi-steady state where steps 1,···,n+1 move right with a smaller constant velocity, V_{n+1}. Since step n+1 increases its velocity from essentially zero to V_{n+1} in a very short time interval, we can still associate a **collision time**, t_n in this non local case, with the time when this sudden change in the velocity of step n+1 occurs. For preciseness, we define t_n as the time at which the velocity of step n+1 is equal to half the velocity of step n. As shown in the **Appendix**, the velocity of steps 1,···,n in the nth quasi-steady state is given by $V_n = D_r\tilde{\mathcal{E}}/n$. In effect, the pressure from the reconstructed facet is divided by the number of steps in the uniformly moving bunch. Therefore, we expect in the nth quasi-steady state interval

$\Delta t_n \approx (w_a - w_b)/V_n = \tilde{w}n/(D_r\tilde{\varepsilon})$ and we have $t_n \approx \tilde{w}n^2/(2D_r\tilde{\varepsilon})$. On the other hand, the width of the zeroth terrace has increased at $t = t_n$ by as much as the widths of terraces 1, 2,···,n have decreased, since the position of step n+1 has hardly changed. Therefore, in the absence of other nucleation events, we have $w_0(t_n) - w_0(t=0) \approx \tilde{w}n \approx 2D_r\tilde{e}\tilde{w}^{1/2}(t_n)^{1/2}$. This exhibits a $t^{1/2}$ dependence in agreement with the classic continuum treatment of Mullins [8].

Figure 6b shows the widths of the first few terraces as a function of time. As discussed above, w_k remains almost constant (initial value, w_a) for $t < t_{k-1}$. For $t_{k-1} < t < t_k$, it decreases linearly to nearly the final step bunch width and then decreases very slowly from that to the final size w_b for $t > t_k$. Since the terraces in the bunch change their width so little after they join the bunch, all steps in the bunch move with essentially the same velocity as assumed in the quasi-steady state approximation. In the zeroth approximation, the width of the kth terrace in front of the growing facet is given by (see **Appendix**)

$$w_k = (1 - \tilde{e}k/n)^{-1/3} w_b \tag{17}$$

for $k = 1,\cdots,n$ where $\tilde{e} = 1 - (w_b/w_a)^3$. For $k > n$, terrace widths remain at their initial value w_a.

Continuum approximation for bunch shape near the facet

As discussed in the local conservation case, this simple zeroth order picture must certainly break down if w_n-1 from Eq. (17) is of order w_a. This break-down occurs in the non local case where $t > t_{n_c}$ with t_{n_c} such that

$$w_{n_c-1}(t_{n_c}) = \left[\frac{n_c}{(1+(p_a/\varepsilon)(n_c-1))}\right]^{1/3} w_b \quad \approx w_a \tag{18}$$

As before, we use scaling arguments and the quasi-steady state solution, Eq. (17) with $n(t) = v^{\dagger}t^{\beta}$, to describe the (long) time dependent shape of the growing step bunch near the facet. This time, we get $\beta = ½$ when we put the scaling $w(k,t) = w(kt^{-\beta})$ in Eq. (6). The terrace widths are now given by

$$\begin{aligned} w(v) &= \left(1 - \tilde{e}k/v^{\dagger}t^{1/2}\right)^{-1/3} w_b \\ &= \left(1 - \tilde{e}v/v^{\dagger}\right)^{-1/3} w_b. \end{aligned} \tag{19}$$

Using the scaling variable $v = kt^{-1/2}$ implies that the profile is described on a scale which increases as $t^{1/2}$. Therefore, it is natural to describe the surface height with a continuous variable, z, at long times. In this limit, Eq. (19) becomes

$$\partial_z x\left(zt^{-\frac{1}{2}}\right) = \left(1 - \tilde{e}zt^{\frac{1}{2}}/v^{\dagger}\right)^{-1/3} w_b \tag{20}$$

or, with scaling variables $u = xt^{-1/2}$ and $v = zt^{-1/2}$,

$$u'(v) = \left(1 - \tilde{e}v/v^{\dagger}\right)^{-1/3} w_b, \tag{21}$$

where $u' = du/dv$. By integrating both sides of the Eq. (21) and by solving it for $z = vt^{1/2}$, we get the surface profile,

$$z(x,t) = t^{1/2}\frac{v^{\dagger}}{\tilde{e}}\left[1 - \left(1 - \frac{2\tilde{e}\left(xt^{-\frac{1}{2}} - u_1\right)}{3w_b v^{\dagger}}\right)^{3/2}\right]. \tag{22}$$

where $u_1 = x_1 t^{-1/2}$ is the rescaled position of the interface between flat reconstructed surface and the step bunch. Note that Eq. (22) is the profile for the step bunch region and hence is valid only for $x_1 < x < x^{\dagger}$ where $x^{\dagger}$ is the end of the step bunch defined by $z(x^{\dagger},t) = v^{\dagger}t^{1/2}$. For $x < x_1$, we have a facet with $z = 0$ from the definition of x_1 while for $x > x^{\dagger}$, the profile is given by the unperturbed initial surface, $z = s_o x$.

Now we need to determine the two constants $v^{\dagger}$ and u_1 in Eq. (22). This equation should describe the profile accurately for $z << z^{\dagger}$, so we require that it satisfy Eq. (6) or the corresponding continuum equation for $\dot{z} \equiv \partial_t z$ **exactly** at x_1. The continuum equation for $\dot{z}$ can be derived easily from Eq. (6) since $\dot{z} = -s\dot{x}$, where $s = z' \equiv \partial_x z$ is the slope of the profile at x;

$$\dot{z} = 2gD_r\partial_x s^3 = 6gD_r z'^2 z''. \tag{23}$$

The self consistency condition at x_1 gives

$$u_1 v^{\dagger} = 2D_r\tilde{\varepsilon}, \tag{24}$$

since $\dot{z}(x_1,t) = -u_1 t^{1/2}/2w_b$ from the definition of u_1. In what follows, we use Eq. (24) to determine $v^{\dagger}$ when different choices are made for u_1.

Surface profiles at different times determined from numerically integrating the discrete equations are shown in Figure 7, using scaling variables $u \equiv xt^{-1/2}$ and $v \equiv zt^{-1/2}$. In Figure 7a, we show surface profiles at four different t_n with n = 10, 15, 30 and 90 for $w_r \equiv w_b/w_a$ = 1/10. Again the scaling ansatz is very accurately obeyed.

These results are compared with the approximate continuous profiles given by Eq. (22), using two different values of u_1 {$v^{\dagger}$ is given by equation (24)}. The dashed line is the case where we directly fit u_1 to the numerical profile at t_{n_4}.

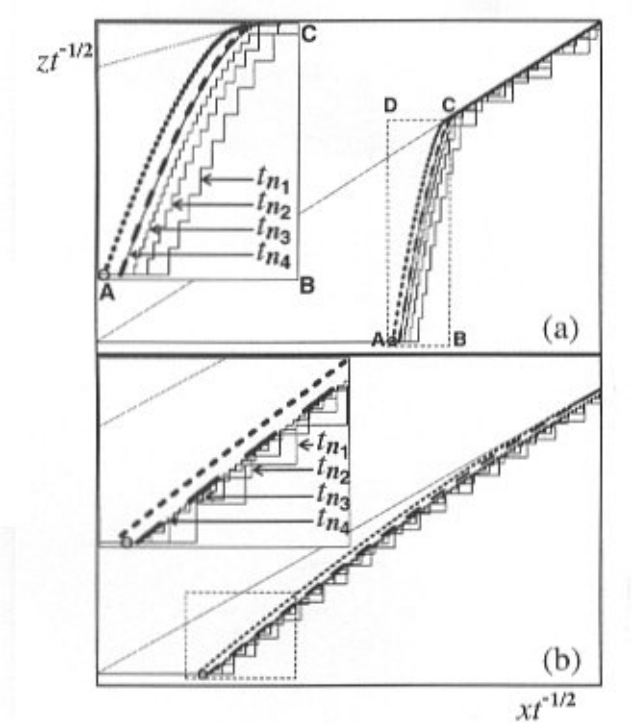

Figure 7. Surface profiles at different times are shown with scaling variables, $u = xt^{-1/2}$ and $v = zt^{-1/2}$ for two different values of w_b/w_a: 1/10 (**a**), and 2/3 (**b**). They are compared with the continuous profiles (dashed lines and dotted lines) given by Eq. (22) with two different values of u_1. The open circle on the u axis represents the extrapolated value (at $t = \infty$) of the rescaled position of the first step. See text for the value of u_1's in the continuous profiles and the definition of the collision time t_{n_i}'s.

We see that two profiles coincide very well almost everywhere with this choice of u_1.

The other continuous profile, the dotted line, is obtained by a crude matching of Eq. (22) at $u^\dagger = x^\dagger t^{-1/2}$ to the **unperturbed** initial profile (the thin solid line), given by $v = u/w_a$. Note that the slope, $s = \partial_x z = v'(u)$ from Eq. (22) is s_a at $u^\dagger$. An approximation to u_1 can be obtained by imposing $v(u^\dagger) = s_a u^\dagger$ and using Eq. (24). In general, this approximation gives a **lower bound** to u_1 since $v^\dagger = v(u^\dagger)$ must be slightly smaller than $s_a u^\dagger$ in real profiles. With this approximation, it is straightforward to calculate u_1 and $v^\dagger$. They are given by

$$u_1 = \left[2D_r \varepsilon w_a \left(1 - \frac{3}{2} w_r + \frac{1}{2} w_r^3 \right) \right]^{1/2}$$
$$v^\dagger = \left(\frac{2D_r \varepsilon}{w_a} \right)^{1/2} \left(1 - w_r^3 \right) \Big/ \left(1 - \frac{3}{2} w_r + \frac{1}{2} w_r^3 \right)^{1/2}. \quad (25)$$

The dotted line is the profile of Eq. (22) with the above u_1 and $v^\dagger$. As we can see in Figure 7, the re-scaled surfaces' profiles at different times approach a single curve as t increases. The open circle represents the limiting value of the rescaled position of the first step, $\lim_{t\to\infty} x_1(t)t^{-1/2}$, which is obtained by an extra-polation. For small w_r, this extrapolated value, and u_1 in Eq. (22), are very close. For example, the difference is less than 0.2% for $w_r < 1/10$. Note that the shapes of rescaled profiles are almost the same (except the degree of discreteness) for different times, especially for large t. Hence, we expect that there would be no noticeable difference between the rescaled profile at $t = \infty$ and the dotted line.

When w_r is not so small, Eq. (22) is inaccurate near $u^\dagger = x^\dagger t^{-1/2}$ but still describes the profile rather well for small v. In Figure 7b, we show surface profiles at four dif-ferent t_n with n = 15, 20, 40 and 80 for w_r = 2/3. As in Figure 7a, they are compared with two continuous profiles, one with u_1 from t_{n_4} and the other using u_1 from Eq. (22). This time, the extrapolated value of u_1 from numerical profiles is slightly larger than the value given by Eq. (25). This discrepancy is understandable since Eq. (22) is invalid near $u^\dagger$ unless $w_r << 1$. Our crude patching of Eq. (22) at $u^\dagger$ with an outer ($u > u^\dagger$) solution of Eq. (23), $v = s_a u$, describing the unperturbed initial profile ($\dot{z} = 0$ for $u > u^\dagger$), is a good approximation only for $w_r \to 0$.

We may be able to develop a more accurate continuum profile if we use a better approximation for the outer solution and an improved matching procedure. For example, we could approximate Eq. (23) by

$$\dot{z} = 6gD_r s_i^2 z'' \quad (26)$$

for the outer region and use the solution [8] for the above equation as the outer solution. Matching it with the inner solution of Eq. (22) over some proper region in $(u_1,u^\dagger)$ could give an improved approximation for the profile over the entire region [1].

Nevertheless, the naive patching using the unperturbed configuration for the outer region, Eq. (25) still seems accurate enough to allow an estimate of some important parameters in the reconstruction driven faceting process. We can estimate (the upper bound of) $D_r\varepsilon$ by measuring the time dependence of the reconstructed facet growth, $x_1(t)$;

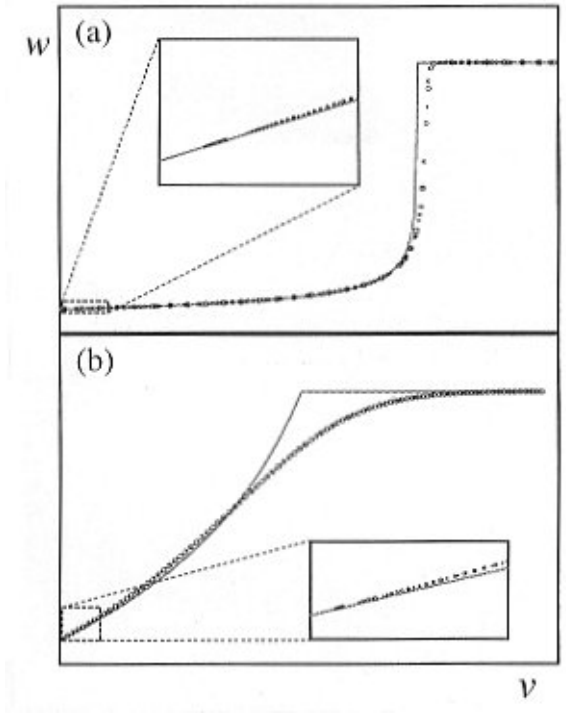

Figure 8. Terrace widths as a function of the scaling variable, $v = kt^{-\beta}$ with $\beta = ½$ for two different values of w_b/w_a: 1/10 (**a**), and 2/3 (**b**). Terrace widths at different times collapse to a single curve for each given w_b/w_a. This curve is compared with Eq. (28). In insets, terrace widths show a linear increase for small v. They are compared with Eq. (29).

$$D_r\varepsilon = \left[\left(1-\frac{3}{2}w_r+\frac{1}{2}w_r^3\right)\right]^{-1/2}\frac{x_1 t^{-1/2}}{2w_a} \qquad (27)$$

from Eq. (25). This value can also be extracted from the profile near the reconstructed facet at later times. As shown in Figure 7, the dotted lines describe the shape of the profile well near $v = 0$ (except for the overall shift) even when w_r is not small. The inverse slope (terrace width) of the dotted lines can be calculated from Eqs. (19) and (25) and is given by

$$w(v) = \left[1-\left(\frac{w_a}{2D_r\varepsilon}\right)^{1/2}\left(1-\frac{3}{2}w_r+\frac{1}{2}w_r^3\right)^{1/2}v\right]^{-1/3} w_b. \qquad (28)$$

We see that it increases linearly for small v;

$$w(v) \approx w_b + \frac{w_b}{3}\left(\frac{w_a}{2D_r\varepsilon}\right)^{1/2}\left(1-\frac{3}{2}w_r+\frac{1}{2}w_r^3\right)^{1/2}v. \qquad (29)$$

In Figure 8 we plot terrace widths (from the numerical integration) versus the scaling variable v. As expected the terrace widths at different times collapse to a single curve. This curve is compared with Eqs. (28) and (29). As shown in the insets, the terrace widths increase linearly with v for small v and the slope is not much different from the value given by Eq. (29). In an experiment, by measuring the terrace widths near the growing facet at sufficiently long times (small v), one can estimate $D_r\varepsilon$ from Eq. (29).

Concluding Remarks

The principal conclusion from this analysis is that a growing nucleus can induce the formation of another nucleus nearby when the mass is conserved locally. This induced nucleation process is analyzed using a detailed surface profile near the growing terrace obtained from a physically suggestive zeroth order picture. The resulting regular order has a purely **kinetic** origin. The long time behavior of the faceting is also obtained from this zeroth order profile using scaling variables. A similar analysis is carried out for the non-conserved case.

For quantitative comparison with experiments, more studies are needed, including a detailed analysis of a 2D model. In particular, the role of thermal fluctuations in the nucleation process needs to be understood better. Work along these lines is underway. However, many of the qualitative predictions of the present 1D model may be tested in experiments. For faceting dominated by induced nucleation, we expect to see the propagation of nucleation and regularity in the faceted surfaces. Also, as shown in Figure 5, we can tell the induced nuclei from the thermally nucleated ones by carefully analyzing the terrace width distribution near the growing facet, since the small v behavior strongly depends on whether there is net flux across the reconstructed terrace.

Appendix

In the zeroth order approximation, for the nth quasi-steady state ($t_{n-1} < t < t_n$), we have

$$\partial_t x_k = \partial_t x_1, \qquad (A1)$$

for $k = 2,\cdots,n$ with a boundary condition $\xi_{n+1} = 0$. The chemical potential given by Eq. (5) can be written as $\xi_k = p_{k-1}-p_k$ where the "pressure" of the kth terrace, $p_k = 2g/w_k^3 + \varepsilon\,\theta(w_k-w_c)$. Since the pressure on the reconstructed terrace is almost equal to ε and the pressure on an unperturbed terrace with width w_a is $2g/w_a^3$ (for $k \geq n$), we have

$$\sum_{i=1}^{n}\xi_i=\sum_{i=1}^{n}\left(p_{k-1}-p_k\right)\quad=p_{k=0}-p_n\quad=\tilde{\varepsilon},\tag{A2}$$

where $\tilde{\varepsilon}=\varepsilon-2g/w_i^3$.

I. With local conservation

For the locally conserved case, the velocity of the steps are given by

$$\partial_t x_n=(2\xi_n-\xi_{n-1}-\xi_{n+1})\tag{I1}$$

where we set $D_s=1$ for convenience. From Eqs. (A1) and (I1), we have: $2(\xi_{k+1}-\xi_k)=(\xi_k-\xi_{k-1})+(\xi_{k+2}-\xi_{k+1})$.

The symmetric case ($\xi_0=-\xi_1$). For a thermally nucleated facet, we expect that the chemical potential at step 0 satisfies ($\xi_0=-\xi_1$) due to symmetry. By solving Eqs. (A1), (A2) and (I1), with this boundary condition, we get

$$\xi_k=\frac{3\tilde{\varepsilon}\left[-(2n+1)k^2+\left(2n^2+4n+1\right)k-n(n+1)\right]}{n\left(n^3+2n^2+2n+1\right)},\tag{I2}$$

and the velocity of steps $k=1,\cdots,n$, V_n is given by

$$V_n=6\tilde{\varepsilon}(2n+1)/\{n(n^3+2n^2+2n+1)\}\tag{I3}$$

The adatom flux $\Phi_l(n)$ moving left from the step $k=1$ to $k=0$ during the nth quasisteady state is given by

$$\Phi_l(n)=(\xi_1-\xi_0)=n(n+1)(2n+1)^{-1}V_n\tag{I4}$$

while the adatom flux moving right from the step $k=n$ to $k=(n+1)$, $\Phi_r(n)$ is $nV_n-\Phi_l(n)$. Since only $\{\Phi_r/(\Phi_l+\Phi_r)\}$ of atoms removed from the terrace k (for $t_{k-1}<t<t_k$) move right, we expect

$$\Delta w_n=\sum_{k=1}^{n-1}\frac{k}{2k+1}\left(\Delta w_k+\tilde{w}-\Delta w_{k+1}\right),\tag{I5}$$

where $\Delta w_n=w_n^{max}-w_a$. In other words, we have a recurrence relation between w_n^{max}'s:

$$w_n^{max}=w_a+\frac{2n-1}{3n-2}\left[\sum_{k=1}^{n-1}\frac{\tilde{w}k}{2k+1}+\sum_{k=2}^{n-1}\frac{w_k^{max}-w_a}{4k^2-1}\right].\tag{I6}$$

Step n moves right with velocity V_n and step n+1 moves left with velocity $n^2V_n/(2n+1)$. The time required for these two neighboring steps to collide is t_n-t_{n-1} and is given by

$$t_n-t_{n-1}=w_n^{max}/\{V_n(1+n^2)/(2n+1)\}.\tag{I7}$$

At t_n, the zeroth terrace width is given by

$$w_0(t=t_n)=w_0(t=0)+\sum_{k=1}^{n}V_{(k)}(t_k-t_{k-1}).\tag{I8}$$

Now, let us consider the asymptotic value of Eqs. (I6), (I7) and (I8) for large t. For large n, $w_n^{max}\approx\tilde{w}n/3$ and $t_n-t_{n-1}\approx\tilde{w}n^3/18\tilde{\varepsilon}$. Thus, the width of the facet increases as

$$\begin{aligned}w_0(t)&=w_0(t=0)+2\sum_{k=1}^{n}V_n(t_n-t_{n-1})\\&\approx\frac{4}{3}(72\tilde{\varepsilon})^{1/4}(\tilde{w})^{3/4}t^{1/4}.\end{aligned}\tag{I9}$$

The factor 2 in front of the second term is from the fact that the facet grows in both directions.

The pressure on the kth terrace is obtained from Eq. (I2):

$$\begin{aligned}p_k&=\varepsilon-\sum_{l=1}^{k}\xi_l\\&=\varepsilon\left[1+h_1(n)k-h_2(n)k^2+h_3(n)k^3\right],\end{aligned}\tag{I10}$$

where

$$\begin{aligned}&h_1(n)=\{3(2n^2+4n+1)-\tfrac{1}{2}(2n+1)-3n(n+1)\}/D(n),\\&h_2(n)=\{3(2n^2+4n+1)-3(2n+1)\}/2D(n),\\&h_3(n)=(2n+1)/2D(n)\end{aligned}\tag{I11}$$

with $D(n)=\tilde{\varepsilon}/\{\varepsilon n(n^3+2n^2+2n+1)\}$. The terrace width, w_k, is now given by

$$w_k=w_b\{1+h_1(n)k-h_2(n)k^2+h_3(n)k^3\}^{-1/3}\tag{I12}$$

Note that both $h_1(n)$ and $h_2(n)$ are proportional to n^{-2} for large n. Therefore, the linear term, $h_1(n)k$, can be ignored in the continuum limit where both n and k go to infinity.

The asymmetric case ($\xi_0=\xi_1$). For the induced nuclei, there is no flux across the reconstructed terrace, hence $\xi_0=\xi_1$. In the steady state, ξ_k should be quadratic in k since $V_k(2\xi_k-\xi_{k+1}-\xi_{k-1})$ is constant for $k=1,\cdots,n$. With the boundary conditions $\xi_0=\xi_1$ and $\xi_{n+1}=0$, the chemical potential at step $k(k\le n)$, ξ_k, for $t_{n-1}<t<t_n$ can be written as

$$\xi_k=a\{k(k-1)-n(n+1)\}\tag{I13}$$

with a constant $a = -3\tilde{\varepsilon}/\{n(n+1)(2n+1)\}$ which is obtained from the constraint, Eq. (A2). Then, the velocity of steps 1,···,*n*, is given by

$$V_n = 6\tilde{\varepsilon}/\{n(n+1)(2n+1)\} \tag{I14}$$

Since *all* atoms from the step $k(k > 0)$ go right in this case, the step n+1 moves left with the velocity, nV_n. Therefore, the recursion relation between the w_n^{max}'s is now given by $w_n^{max} = w_a + (n\text{-}1)(w_{n-1}^{max} - w_b)/n$, and from $w_1^{max} = w_a$ we have

$$w_n^{max} = w_a + \{(n\text{-}1)/2\}\tilde{w} \tag{I15}$$

This result can be understood easily from the fact the w_0 and w_n^{max} are the same in the $\xi_0 = \xi_1$ case. Since the position of the step n+1 is not changed at t_{n-1}, we have $w_0 + w_n^{max} = 2w_a + (n\text{-}1)(w_a\text{-}w_b)$. From $w_0 = w_n^{max}$, we get $w_n^{max} = w_a + \{(n\text{-}1)/2\}\tilde{w}$. Step n moves right with velocity V_n and step n+1 moves left with velocity nV_n. The time required for these two neighboring steps to collide, $\Delta t_n = t_n\text{-}t_{n-1}$, is given by

$$\begin{aligned} \Delta t_n &= w_n^{max}/\{(n+1)V_n\} \\ &= \{n(2n+1)/6\tilde{\varepsilon}\}\cdot\{w_0+\{(n\text{-}1)/2\}\tilde{w}\} \\ &\approx (\tilde{w}/6\tilde{\varepsilon})n^3 \end{aligned} \tag{I16}$$

Hence, t_n is given by $t_n \approx (24\tilde{\varepsilon}/\tilde{w})^{1/4}$

The pressure and the terrace widths are obtained again from the chemical potential. From Eq. (I13),

$$\begin{aligned} p_k &= \varepsilon - \frac{3\tilde{\varepsilon}k}{2n+1} + \frac{\tilde{\varepsilon}k\left(k^2-1\right)}{n(n+1)(2n+1)} \\ &= \varepsilon\left[1 - \frac{\left(3n^2+3n+1\right)\tilde{e}\,k}{n(n+1)(2n+1)} + \frac{\tilde{e}\,k^3}{n(n+1)(2n+1)}\right] \end{aligned} \tag{I17}$$

where $\tilde{e} = \tilde{\varepsilon}/\varepsilon$ and the terrace width, w_k, is given by

$$w_k = w_b\left[1 - \frac{\left(3n^2+3n+1\right)\tilde{e}\,k}{n(n+1)(2n+1)} + \frac{\tilde{e}\,k^3}{n(n+1)(2n+1)}\right]^{-1/3}. \tag{I18}$$

II. Without Local Conservation

In the non-conserved case, the velocity of the steps are given by $\partial_t x_k = \xi_k$, where we set the diffusion constant $D_r = 1$ for simplicity. For the nth quasi-steady state ($t_{n-1} < t < t_n$), we have

$$\partial_t x_k = \xi_k = \tilde{\varepsilon}/n \tag{II1}$$

for $k \le n$, from Eq. (A1) and (A2) with the boundary condition $\xi_{n+1} = 0$. Since $t_n\text{-}t_{n-1}$ is the time required for the nth terrace to shrink to w_b from w_a, $t_n\text{-}t_{n-1} = n\tilde{w}/\tilde{\varepsilon}$, where $\tilde{w} = w_a\text{-}w_b$. At t_n, the zeroth terrace width, $w_0(t=t_n) \approx w_0(t=0)+n\tilde{w}$, where $t_n = \Sigma_{=1}\,(t_i\text{-}t_{i-1}) = n(n+1)\tilde{w}/2\tilde{\varepsilon}$. Therefore, we have

$$w_0(t=t_n) \approx w_0(t=0) + 2(2\tilde{\varepsilon}\tilde{w})^{1/2}t^{1/2} \tag{II2}$$

From $\xi_k = \tilde{\varepsilon}/n$, the pressure and width of the kth terrace are given by

$$\begin{aligned} p_k &= \{p_0\text{-}(k/n)\tilde{\varepsilon}\} = \varepsilon\{1\text{-}(\tilde{\varepsilon}k/\varepsilon n)\} \\ w_k &= (p_k/2g)^{-1/3} = w_b\{1\text{-}(\tilde{\varepsilon}k/\varepsilon n)\}^{-1/3} \end{aligned} \tag{II3}$$

for $k < n$. For $k \ge n$, terraces have the initial average width and pressure, w_a and p_a.

Acknowledgements

We are grateful to D. J. Liu, J.E. Reutt-Robey, and E.D. Williams for helpful discussions and M.G. Spell for excellent mauscript preparation. This work was supported by the NSF MRG with continuing support from the NSF MRSEC under contract DMR 96 32521.

References

[1] Bender CM, Orszag SA (1978) Advanced Mathematical Methods for Scientists and Engineers. McGraw-Hill, New York. p. 426.

[2] Gruber EE, Mullins WW (1967) On the theory of anisotropy of crystalline surface tension. J. Phys. Chem. Solids **28**, 875–887.

[3] Heffelfinger JR, Bench MW, Carter CB (1995) On the faceting of ceramic surfaces. Surf. Sci. **343**, L1161–L1166.

[4] Hibino H, Homma Y, Ogino T (1995) Real space observation of (111) facet formation on vicinal Si(111) surfaces. Phys. Rev. B **51**, 7753–7761.

[5] Jayaprakash C, Rottman C, Saam WF (1984) Simple model for crystal shapes: Step step interactions and facet edges. Phys. Rev. B **30**, 6549–6554.

[6] Jeong HC, Weeks JD (1995) Faceting through the propagation of nucleation. Phys. Rev. Lett. **75**, 4456–4459.

[7] Joós B, Einstein TL, Bartelt NC (1991) Distribution of terrace widths on a vicinal surface within the one-dimensional free fermion model. Phys. Rev. B **43**, 8153–8162.

[8] Mullins WW (1957) Theory of thermal grooving. J. Appl. Phys. **28**, 333–339.

[9] Nozières P (1987) On the motion of steps on a vicinal surface. J. Phys. France **48**, 1605–1608.

[10] Nozières P (1992) Shape and growth of crystals. In: Solids far from equilibrium. Godrèche C (ed.). Cambridge University Press, Cambridge, U.K. pp. 1–154.

[11] Ozcomert JS, Pai WW, Bartelt NC, Reutt-Robey JE (1994) Kinetics of oxygen induced faceting of vicinal Ag(110). Phys. Rev. Lett. **72**, 258–261.

[12] Phaneuf RJ, Bartelt NC, Williams ED, Œwiech W, Bauer E (1991) Low energy electron-microscopy investigations

of orientational phase separation on vicinal Si(111) surfaces. Phys. Rev. Lett. **67**, 2986–2989.

[13] Phaneuf RJ, Bartelt NC, Williams ED, Œwiech W, Bauer E (1993) Crossover from metastable to unstable facet growth on Si(111). Phys. Rev. Lett. **71**, 2284– 2287.

[14] Pokrovsky VL, Talapov AL (1979) Ground state, spectrum, and phase diagram of two dimensional incomsurate crystals. Phys. Rev. Lett. **42**, 65–67.

[15] Pourmir F, Rousset S, Gauthier S, Sotto M, Klein J, Lecoeur J (1995) Superperiodicity in the thermal faceting of Au(111) vicinal surfaces. Surf. Sci. **324**, L337– L342.

[16] Rettori A, Villain J (1988) Flattening of grooves on a crystal surface: A method of investigation of surface roughness. J. Phys. France **49**, 257-267.

[17] Williams ED, Bartelt NC (1991) Thermodynamics of surface morphology. Science **251**, 393–400.

[18] Williams ED, Bartelt NC (1996) Thermodynamics and statistical mechanics of surfaces. In: Handbook of Surface Science, Vol. I, Physical Structure. Unertl WN (ed.). Elsevier Science, Amsterdam, Netherlands. pp. 51-99.

[19] Yoon M, Mochrie SGJ, Zehner DM, Watson GM, Gibbs D (1995) Periodic step bunching on a miscut Pt(111) surface. Surf. Sci. **338**, 225–235.

Discussion with Reviewers

N.C. Bartelt: The use of a 1D model is justified by referring to experimental observations of linear facet edges of Si(111). I would argue that this is slightly dangerous because the spectacular linearity on Si(111) is probably associated with (elastic) effects not included in the authors' model. Can the 1D model be justified more generally?

Authors: Indeed, surface elasticity has a strong influence on the surface morphology of the Si(111) faceted surface, and probably produces the extreme linearity of the facet edges as noted above. However, rather linear facet edges have been found in several other systems, including GaAs(001) and O/Ag(110), not all of which exhibit strong surface elasticity effects. An elongated, rather linear facet edge is expected in general if faceting occurs through nucleation of reconstructed regions since the reconstruction propagates asymptotically much faster ($\sim t$) in the direction parallel to the step edge than in the perpendicular direction ($\sim t^{1/2}$ or $t^{1/4}$). We believe that the 1D variable, the averaged position of the step over these linear regions would properly describe the faceting process on a scale smaller than the lateral size of the facet. The validity of using the 1D free energy, Eq. (4), has not been shown rigorously but the result of 2D numerical models seems to agree with the 1D free energy.

N.C. Bartelt: The authors use the free fermion distribution of terrace widths to determine the smoothing of the cusp in the free energy. When g is large (as it is on Si(111), for example), the distribution can be much smaller than this. So the authors are probably over-estimating the smoothing of the cusp. However, in the sections **Model** and **Kinetics** it is argued that the smoothed free-energy curve is not what one should use in the calculation of the step dynamics. What, then should one use the smoothed free-energy curve for? Is it physically meaningful?

Authors: The free energy one should use depends on the time and spatial scale on which the system is to be described. The long time behavior of the system can be described using the true equilibrium free energy, which is the lower envelope of the thick curves. It predicts the phase separation and the properties of each phase. The smoothed curve in Figure 1b represents a hypothetical (non-equilibrium) free energy of the system at the moment the reconstruction is allowed (e.g., when the system is quenched below the reconstruction temperature) with instantaneous reconstruction occurring on sufficiently wide terraces. If the system is well described by a local slope, coarse-grained over several terraces, which might be the case in the spinodal decomcosition regime, the short time dynamics might be more appropriately described by the smoothed free energy curve. However, for the motion of individual (linear) steps on a scale smaller than lateral facet size as considered here, the cusped free energy in Figure 1a is the one we should use.

N.C. Bartelt: One of the most interesting conclusions of this work is the periodicity of the final faceted state in the case of conserved dynamics. From the authors results, is it possible to give a qualitative discussion about how the final periodicity depends on the parameters of the problem? For example, how sensitive is the periodicity to the magnitude of the step step interactions?

Authors: The final periodicity dependence on the parameters are given in Eq. (10) (and below) in the limit of the zeroth order approximation. In this limit, the periodicity mainly depends on the ratio between the critical width and the average width of the terrace (w_c/w_a). We do not have a quantitative analysis for the predicted periodicity when the zeroth approximation is not valid. In this more general case, we believe that the effects of thermal fluctuations are so important that the numerical predictions of our 1D model, which does not permit additional thermal nucleation, are not very meaningful. In fact, the numerically predicted periodicity of the 1D model is quite different from that of a 2D model where thermal nucleation can take place. The periodicity is much smaller and less sensitive to step step interactions in the 2D model. The results of the 2D model will be discussed elsewhere.